Ultrathin Ni layers grown epitaxially on SiC(0001) at room temperature

Y. Hoshino[1,2*], S. Matsumoto[1], and Y. Kido[1]

Abstract

Ultrathin (1-20 ML) Ni layers deposited on 6*H*-SiC(0001)- $\sqrt{3}\times\sqrt{3}$ at room temperature (RT) were analyzed *in situ* high-resolution medium energy scattering (MEIS), reflection high-energy electron diffraction (RHEED), and photoelectron spectroscopy using synchrotron-radiation light. For a Ni coverage of more than 3 ML [1ML for SiC(0001): 1.21×10^{15} atoms/cm^2] uniform Ni(111) layers grow epitaxially at RT in spite of a large lattice mismatch of 20 %. There are two domains, (A) Ni-[110]//SiC[1120] and (B) Ni-[112]//SiC-[1120], and the occupation ratio of (A) to (B) is 5:1. The ion shadowing effect reveals significant expansion of the interplanar distance of Ni(111), which relaxes with increase the Ni thickness. The MEIS analysis shows that a small amount of Si segregate to the surface and the crystalline Ni(111) layer contains Si atoms (3-15 at.%). The segregation rate is derived to be 0.015 s^{-1} by solving a simple rate equation. The uniform stack and epitaxial growth of Ni layers at RT may be responsible for the surface-segregating Si atoms as a surfactant. The two components from Si on top and in the Ni layer are clearly observed in the Si 2*p* spectra and a higher binding energy shift of the latter relative to the former indicates an electronic charge transfer from Si to Ni. The binding energy shift of the Si 2p level of the bulk SiC gives the Schottky barrier height, which reaches the Schottky limit for a thickness above 3 ML.

[1] *Department of Physics, Ritsumeikan University, Kusatsu, Shiga 525-8577, Japan*

[2] *Department of Electronic Science and Engineering, Kyoto University, Nishikyo-ku, Kyoto 610-8510, Japan*

[*] email: yht23389@se.ritsumei.ac.jp

I. INTRODUCTION

Silicon carbide (SiC) is a promising material for its application for high temperature, high power, and high frequency electronic and optoelectronic devices. Recently, Schottky-barrier type diodes are commercially available. Needless to say, metal/SiC contact is of great importance for device fabrication. Unfortunately, the quantitative information is quite insufficient concerning the initial growth process of metal layers on a clean SiC surface and the interfacial reactions between metal and SiC.

In this work, ultrathin Ni layers deposited on the 6*H*-SiC(0001)-$\sqrt{3}\times\sqrt{3}$ surface[1,2] are analyzed *in situ* by reflection high-energy electron diffraction (RHEED), medium energy ion scattering (MEIS), and photoelectron spectroscopy (PES) using synchrotron-radiation (SR) light. RHEED provides information about the structure and crystallinity of stacking Ni layers and MEIS and PES give elemental depth profiles and information on chemical bonds, respectively. A high-resolution toroidal electrostatic analyzer (ESA) makes it possible to determine the Ni thickness and its fluctuation with a resolution of 0.1 nm. In addition, the ion shadowing effect allows one to estimate the structure and crystalline quality of the stacked Ni layers. The Ni/SiC contact generates a band bending, which would depend on Ni thickness. The valence band and Si *2p* core level spectra give the Schottky barrier height attributed to the band bending. The present study revels that Ni(111) layers are grown epitaxially even at room temperature (RT) on a clean 6*H*-SiC(0001)-$\sqrt{3}\times\sqrt{3}$ surface in spite of a large lattice mismatch of 20 %. What makes it possible to stack the Ni layer uniformly and epitaxially on SiC(0001)? The high-resolution MEIS, RHEED, and SR-PES analyses clarify the growth process associated with the interfacial reaction and kinetics for ultrathin Ni layers stacked on the clean SiC(0001) surface.

II. EXPERIMENT

The experiment was carried out at the beamline 8 named SORIS at Ritsumeikan SR Center [3]. It combines MEIS, SR-PES, and a molecular beam epitaxy (MBE) device equipped with RHEED and thus allows an *in situ* analysis under an ultrahigh vacuum (UHV) condition ($<2\times10^{-10}$ Torr). The toroidal ESA used in the MEIS experiment has an excellent energy resolution ($\Delta E/E$) of 9×10^{-4}, which allows a layer-by-layer analysis [4,5]. The present MEIS analysis gives elemental depth profiles, absolute amounts of inclusions, and quantitative evaluation of the crystallinity of the stacked Ni layers. Complementally, SR-PES provides the quantitative information on the chemical bonds and electronic properties. Two types of gratings cover the photon energy from 10 up to 500 eV and the incident photon energies were calibrated by the second and third harmonic waves of SR light. Emitted photoelectrons were analyzed by a hemispherical ESA with a total energy resolution (ΔE) of 150 meV (including Doppler broadening of ~ 100 meV at RT).

The substrates used were N-doped (1.0×10^{18} atoms/cm^3) 6*H*-SiC(0001), whose surfaces

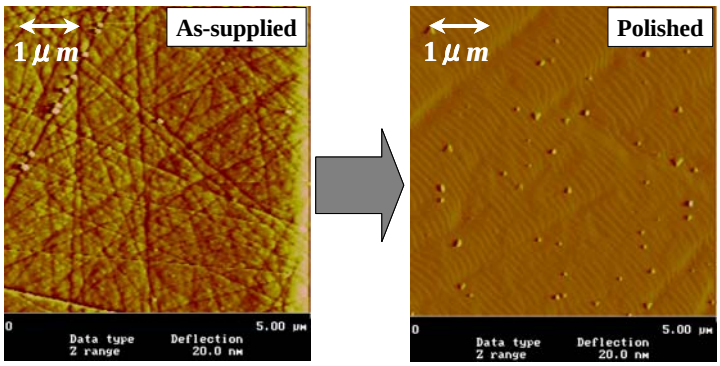

Fig. 1: AFM images observed for 6H-SiC(0001) surfaces as supplied (left) and mechanically polished (right), which underwent same chemical and thermal treatments mentioned in the text.

were polished with colloidal silica (particle size: 0.1 μm) for 10 h followed by the sequential RCA cleaning [6]. Then the substrate was introduced into an UHV chamber and degassed at 600˚C for 5 h with infrared radiation. After being cooled down to RT, Si was deposited about 2.5 ML (1ML for 6*H*-SiC(0001): 1.21×10^{15}atoms/cm^2) with MBE to suppress graphitization of the surface. Finally, the SiC substrate was heated to 1000˚C for 5 min. The surface morphology was observed *ex situ* by an atomic force microscope (AFM) in the atmosphere. Figure 1 shows the AFM images observed for the 6*H*-SiC(0001) as-supplied (left) and mechanically polished (right), whose surfaces underwent same chemical and thermal treatments mentioned above. For the polished surface, the terraces were flat and narrow (≤1000 Å) and a fuzzy image of polishing scratches was still seen. The small particles seen for both surfaces are Si droplets survived and assembled after Si deposition followed by annealing in UHV. Some triangular shape islands observed for the polished surface are fine SiC crystallites survived after heating the Si deposited surface at 1000˚C. We confirmed the clean $\sqrt{3}\times\sqrt{3}$ surface by observation of RHEED and valence band spectra. Ni deposition was performed with a Knudsen cell at a rate of 0.1ML/min and 1.0ML/min, respectively for Ni coverage less than 3 ML and for higher coverage. The absolute amount of Ni coverage was calibrated in advance by Rutherford backscattering using 2.0 MeV He^+ beams.

III. RESULTS AND DISCUSSION

Figure 2 shows the RHEED images taken at the SiC-[1100]- and SiC- [1120]-azimuth for Ni(5ML) as-deposited SiC(0001). Strong and broad streaky lines originating from Ni(111) are seen for both directions, which are ascribed to a uniform stack of Ni layers with small and directional crystal domains. From the RHEED intensity observed at the

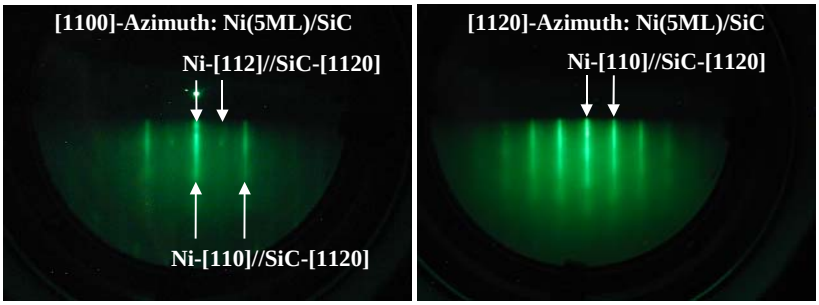

Fig.2: RHEED patterns observed at the [1100] azimuth (left) and at the [1120] azimuth (right) for a Ni deposition of 5 ML at RT on 6H-SiC(0001)

[1100]-azimuth, the domains of Ni(111) whose [110]-axis is parallel to the SiC-[1120] axis (A) are dominant and a small fraction of Ni(111) domains rotated by 90° about the [111]-axis (B) is also seen.

The crystallinity of the Ni-layers stacked at RT was evaluated by MEIS using 120 keV He^+ ions. Figure 3 (right) shows the random and aligned MEIS spectra observed for the SiC(0001) deposited with 10 ML Ni at RT. Considerable reduction of the scattering yield of the aligned spectrum compared with that of the random one indicates an epitaxial growth of the Ni-layer. In this case, the χ_{min} value is estimated to be 0.2. The shape of the rear edge guarantees no strains at the interface. RHEED and MEIS measurements show that the as-deposited Ni-layer with thickness of 1 ML is almost uniform and amorphous [7] and the thicker the Ni layer, the more crystallinity is graded up. It is surprising to see such an epitaxial growth of Ni layers at RT in spite of a large lattice mismatch of 20 %. The best crystallinity is obtained for a Ni coverage around 10 ML and the occupation ratio of the domain (A) to domain (B) is 5 : 1. Figure 3 (left) shows polar-scan spectra at the SiC-[1120] azimuth for He^+ ions scattered from Ni (top and middle) and from Si of SiC(bottom). The angles giving the scattering yield minima are shifted toward a smaller polar angle compared with the ideal [100]-axis of Ni(111). Here, the polar angle of 54.65° ($[\,04\bar{4}1\,]$-axis corresponds to [100]-axis, if 6*H*-SiC is assumed to be cubic) scaled from the surface normal is taken as the basis. In fact, 6*H*-SiC is almost cubic with lattice constant of a = 3.08 Å and c = 15.12 Å (perfectly cubic, if c = 15.09 Å). Such an angular shift means an outward expansion of the Ni(111) plane in the normal direction and shows that the greater the Ni coverage the smaller the expansion. As shown later, the epitaxial Ni layer contains Si atoms with an average concentration of 3-15 at.%. The Si concentration in the Ni layer decreases with increasing Ni coverage. Such Si inclusion may cause the normal expansion of the stacked

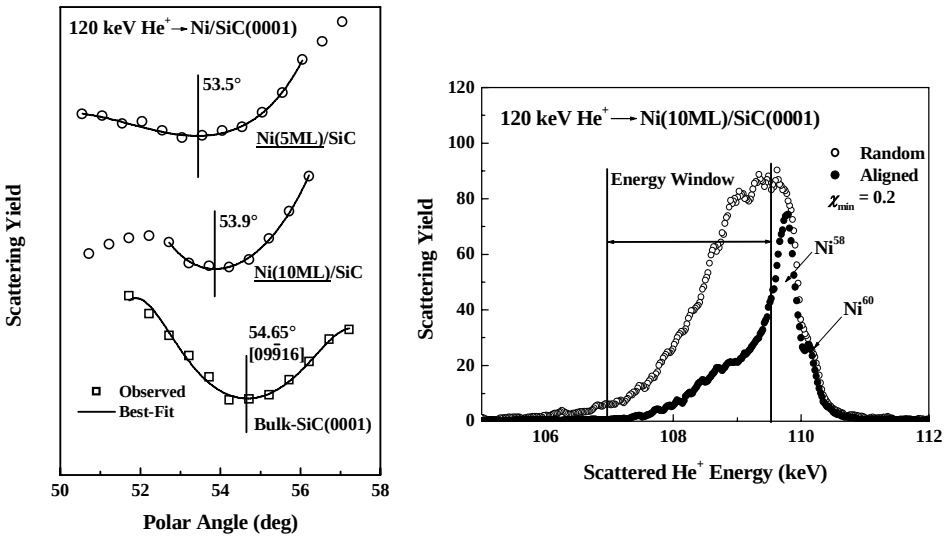

Fig. 3: Random and aligned MEIS spectra (right) observed for 120 keV He+ incident on Ni(10ML)/SiC(0001) and backscattered to 72°. Polar scan spectra at the [112] azimuth (left) for the scattering components from the second- to fifth-layer Ni of Ni(5ML)/SiC (upper), from the second- to tenth-layer Ni of Ni(10ML)/SiC (middle), and from the bulk Si of the SiC substrate (bottom).

Ni(111) layers.

Figure 4 shows the aligned MEIS spectra observed for Ni/SiC(0001) with Ni coverage of 1, 5, and 10ML. Here, it must be noted that a thickness of 10 ML on the basis of SiC(0001) corresponds to 6.5ML on the basis of Ni(111). As expected for an extremely low deposition rate, the Ni layers stack uniformly on the 6*H*-SiC(0001) substrates at RT. For Ni coverage of 1 ML, Si atoms are located below the Ni layer [7], because no sharp peak originating from the surface-segregated Si was observed in the Si *2p* spectrum, which will be discussed later. For higher Ni coverages, however, a small amount of Si is segregated to the surface. The Si surface peak does not come from the uncovered SiC substrate, because the SiC-1×1-RHEED pattern was completely disappeared for Ni coverages above 5 ML and the AFM observation showed uniform surfaces without islands. The Si-surface peak intensity gives 0.4 ML of Si on top of the surface for a Ni coverage of 5 ML. Figure 5 (a) shows the magnified MEIS spectra from Si observed and best-fitted for Ni-coverage of 10 ML. The best-fitting condition gives the Si depth profile as indicated in Fig. 5 (b). Here,

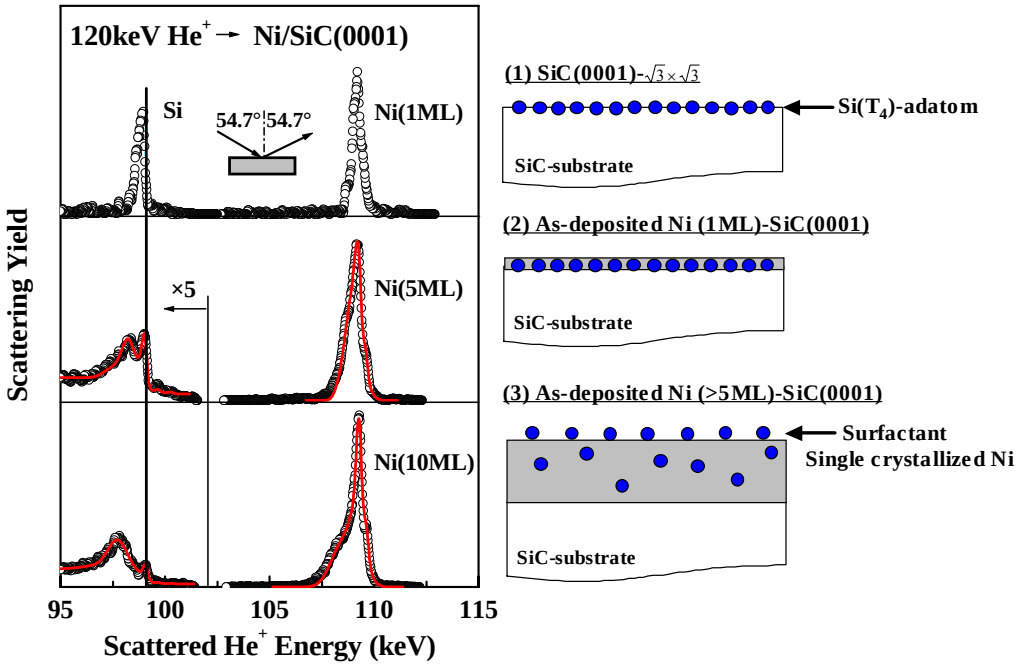

Fig. 4: Aligned MEIS spectra (left) from Ni(1ML) (upper), Ni(5ML) (middle), and Ni(10ML) (bottom) deposited on SiC(0001). Solid curves are the best-fitted spectra assuming appropriate elemental depth profiles and crystallinity of the Ni-layer. Thick straight line indicates the energy position for the scattering component from Si located at surface. (Right) Si atoms contained in Ni-layer and segregated to surface.

we note that 1 ML of Ni(111) corresponds to 1.86×10^{15}atoms/cm^2. The rapid increase in Si concentration near the Ni/SiC interface is a little bit ambiguous because the exact energy straggling is unknown. A precise analysis of the MEIS spectra shows that the Ni layer contains Si atoms with average concentration ranging from 3±1 at.% (Ni-20ML) to15±3 at.% (Ni-3ML). The situation expected from the above MEIS analysis is illustrated in Figure 4 (right).

The total amount of Si located on-top and in the Ni layer is slightly increased with increasing Ni coverage, but almost constant (N_0: $(1.3\pm0.3)\times10^{15}$atoms/cm^2) within experimental error. It is compatible with the amount of the Si atoms of the $\sqrt{3}\times\sqrt{3}$ -adlayer (0.33ML) and of the top Si-C bilayer (1ML). If one assumes that diffusion of Si is allowed only from the second layer to the topmost layer of the growing Ni layer, the amount of the segregated Si (n_1) after the growth of m ML of Ni is expressed by

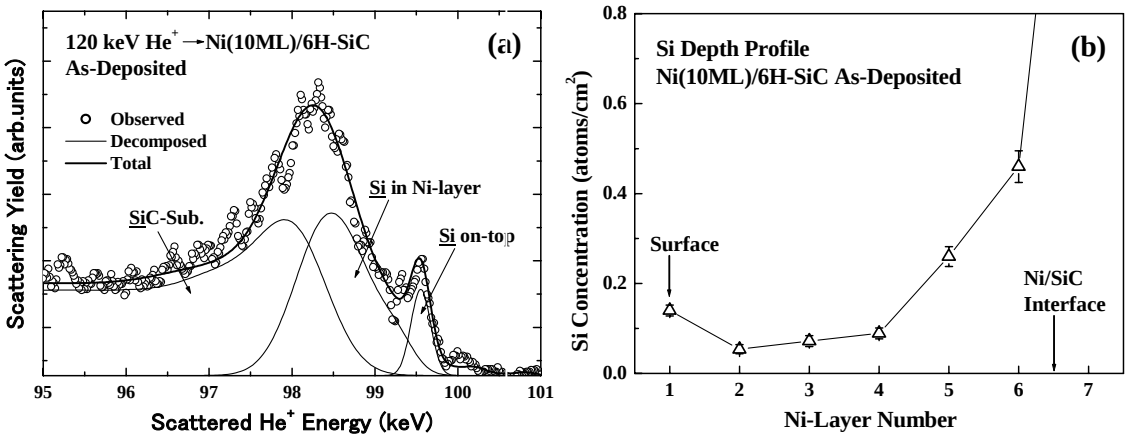

Fig. 5: (a) Magnified MEIS spectra from Si observed (circles) and best fitted (solid curves) for a Ni coverage of 10 ML. (b) Si depth profile derived from the above best-fitting condition. The areal density of Ni(111) is 1.86×10^{15} atoms/cm^2.

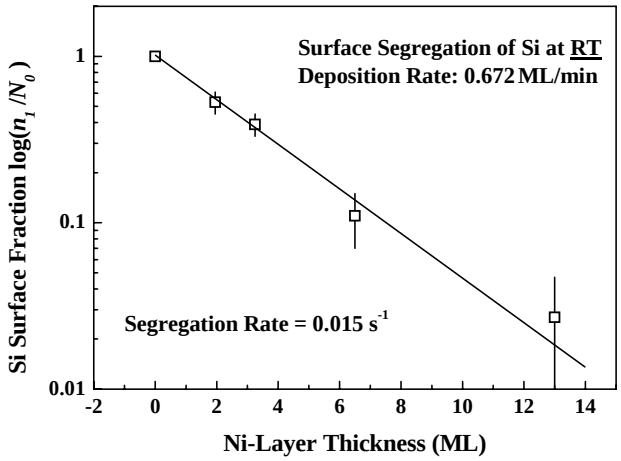

Fig. 6: Ratio of surface-segregated Si atoms (n_1) to total Si atoms released from the SiC surface (N_0) as a function of the Ni coverage m.

$$n_1 = N_0\{1 - exp(-r_s \cdot \tau)\}^m, \qquad (1)$$

where τ and r_s are a growth time of one ML(Ni) and segregation rate, respectively. Here, we regard the continuous growth of the Ni layer as a series of discrete growth steps of one ML each. If one puts the τ value of 89 s and the n_1 values derived by MEIS for Ni coverage of 3, 5, 10, and 20 ML, one obtains the r_s value of 0.015 s^{-1}. Figure 6 indicates the $log_{10}(n_1 / N_0)$ values as a function of Ni coverage m. The slope of the least-square-fitted straight line corresponds to $log_{10}(1 - exp[-r_s \cdot \tau])$. Kimura *et al.*[8] reported that the segregation rate was 0.19 s^{-1} at 130˚C for Sb δ-doped into Si. As is well known, Sb is a representative surfactant for Si homoepitaxy and Ge/Si heteroepitaxy [9]. Such a

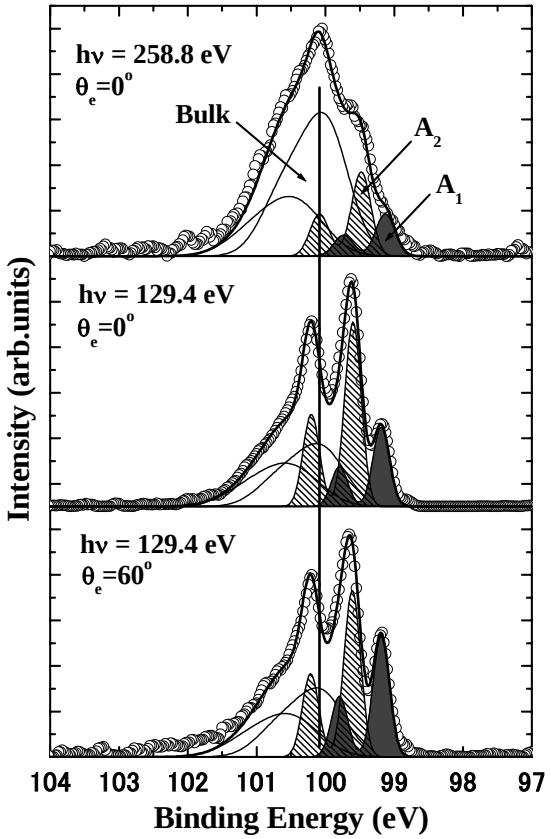

Fig. 7: . Si $2p_{1/2,3/2}$ core level spectra taken for Ni(5ML)/SiC at photon energy of 258.8 eV (2nd harmonic) and at $\theta_e = 0^\circ$(upper), aphoton energy of 129.4 eV and at $\theta_e = 0^\circ$(middle), and at photon energy of 129.4 eV and at $\theta_e = 60^\circ$(bottom). Here, θ_e is emission angle scaled from surface normal. Thick straight line indicates the energy position for the bulk Si $2p_{3/2}$ of the substrate SiC.

surfactantlike behavior of Si plays an important role in stacking uniform and epitaxial Ni layers on SiC(0001) in spite of a large lattice mismatch. It is worth noting that the epitaxial temperatures for MBE growth of Si on Si(001) and Si(111) are 100-300˚C and 400-600˚C, respectively [10].

Figure 7 shows the Si $2p_{1/2,3/2}$ core level spectra taken at photon energies of 129.4 and 258.8 eV(second harmonic) for Ni(5ML)-deposited SiC(0001). First, the energy position of the two sharp components indicated by A_1 and A_2 are determined and then the energy position of the bulk SiC is assigned from the spectrum observed with the second harmonic light giving a larger escape depth. The spectrum deconvolution was performed assuming a Gaussian shape, the spin-orbit splitting of 602 meV [11], and the branching ratio of 1/2. Here, the binding energy is scaled from the Fermi level. The experimental condition becomes more surface sensitive from the top to bottom in Fig. 7. Apparently, the peak A_1 is most surface

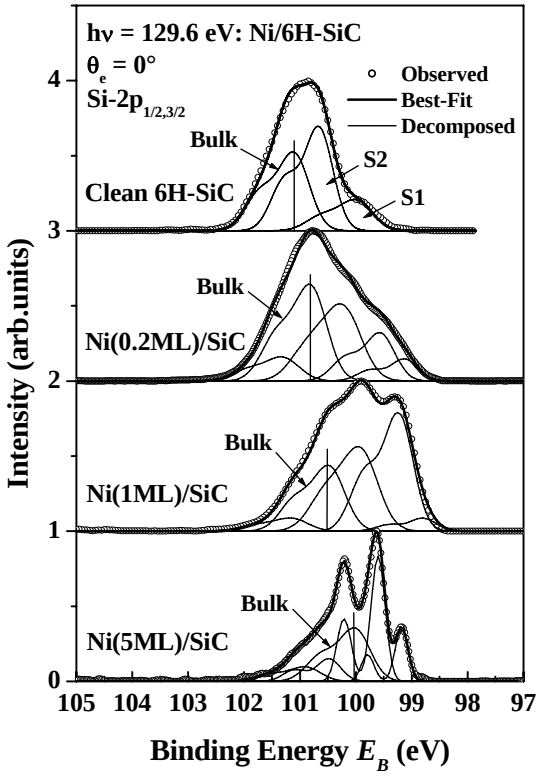

Fig. 8: $2p_{1/2,3/2}$ core level spectra taken at photon energy of 130 eV with normal emission. Samples analyzed are clean 6H-SiC(0001), Ni(0.2ML)/SiC, Ni(1ML)/SiC, Ni(5ML)/SiC from the top to bottom, respectively. S1 and S2 are the surface-related components[14].

sensitive. Considering the previous MEIS result, the components A_1 and A_2 originate from the Si atoms segregated to the surface and located in the Ni layer, respectively. The binding energy and Gaussian width (parenthesis) for the Si $2p_{3/2}$ level for A_1, A_2, and the bulk SiC are

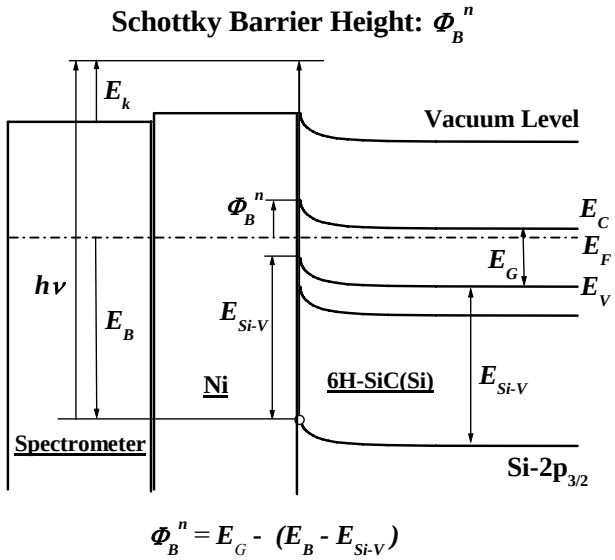

Fig.9 : Schematic diagram of photoemission process. The sample of metal/n-type- SiC is irradiated with photons of known energy, $h\nu$ and electrons (Si $2p$) of binding energy E_B are ejected with a kinetic energy of E_K, which is measured by a spectrometer. The dot-and-dashed line indicates the Fermi level E_F.

99.2 (0.27±0.02), and 99.6 (0.30±0.05), and 100.0 (0.70±0.05) eV, respectively. The line widths observed for the bulk Si and $NiSi_2$ are 0.47 and 0.40 eV, respectively. Considering the total energy resolution of 0.1 - 0.15 eV, the A_1 and A_2 lines are very sharp and thus it suggests the Si atoms dispersed uniformly on the surface and also in the Ni layer, namely very weak Si-Si and Si-Ni interactions. The Si atoms in the Ni layer probably take interstitial sites and weakly interact with the Ni lattice. Almost all the Si atoms in the Ni layer are segregated to the surface by heating at 400˚C. Ni-silicide formation occurs at temperature higher than 450˚C. The higher binding energy shift of A_2 compared with A_1 is due to an electronic charge transfer from Si to Ni. We measured the binding energy of Si $2p_{3/2}$ for a standard sample of $NiSi_2$(13Å)/Si(111) using Al $K\alpha$ X ray (1486.6 eV), which gives a large escape depth. As a result, the binding energies of Si $2p_{3/2}$ for $NiSi_2$ and Si(111) substrate are derived to be 100.0±0.15 and 99.5±0.15 eV, respectively. So, the peaks A1 and A2, respectively seem to originate from Si and Ni-silicide. However, it must be noted that the

as-deposited Ni layers exist, forming the Ni(111) lattice, although it is slightly expanded. Such a charge transfer is not simply explained by comparing the electronegativity of Si (1.74) with that of Ni (1.75). Recently, Liu *et al*.[12] observed chemical shifts of Si *Kα* lines for Fe-Si binary system and found charge transfer from Si to Fe. This is in conflict with the fact that the electronegativity of Fe (1.64) is significantly smaller than that of Si. An *ab initio* full-potential linearized augmented-plane-wave calculation [13] was performed for FeSi and $FeSi_2$ and concluded that in $FeSi_2$, Si lost 0.13 electron to Fe and in FeSi, Si lost 0.18 electron to Fe. The binding energy shifts of Si 2p for Si incorporated in Ni layers would be explained quantitatively by fully quantum mechanical treatments.

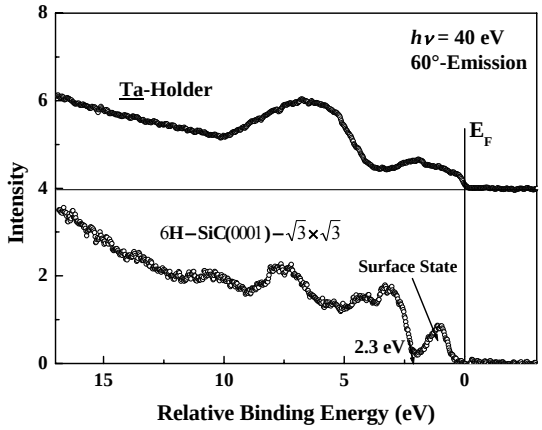

Fig. 10 : Valence band spectra taken at photon energy of 40 eV for Ta-sample holder (upper) and clean 6H-SiC(0001)- $\sqrt{3}\times\sqrt{3}$ surface (lower). Emission angle was set to 60˚ with respect to surface normal. The arrow indicates the position of the valence band maximum.

We observed the Si *2p* spectra for Ni coverages of 0.2, 1.0, 3.0, and 5.0 ML on 6*H*-SiC(0001), as shown in Fig. 8. The bulk Si $2p_{3/2}$ binding energy (E_B) is shifted toward a lower energy side with increasing the Ni-thickness. Such a lower binding energy shift (ΔE_B) reflects an upward band bending at the Ni/SiC interface. Figure 9 shows, schematically, the electronic energy levels at a metal/n-type-semiconductor interface. It should be noted that in general the band of an n-type semiconductor is bent upward up to the surface to satisfy charge neutrality. Semiconductors have surface states originating from dangling bonds and adatom-induced dipoles irrespective of the doping type. The surface states exist in the band gap and act as an acceptor. Thus for n-type semiconductors, the partially filled surface states charged negatively compensate the positive charge of th

The Schottky barrier height (SBH) for n-type semiconductors is given by e ionized donor impurity atoms. It leads to an upward band bending.

$$\Phi_B{}^n = E_G - (E_B - E_{Si-V}) = E_G - E_{VF} + \Delta E_B, \quad (2)$$

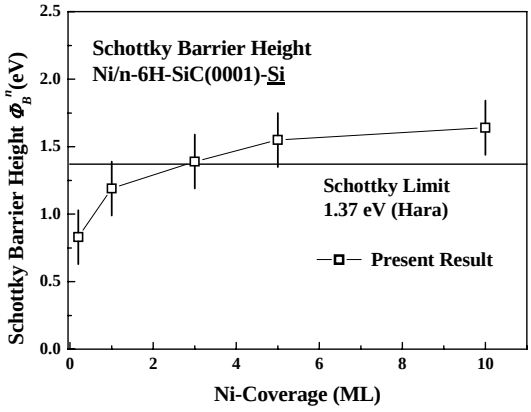

Fig. 11: Schottky barrier heights derived from the Si *2p* core level analysis as a function of Ni-coverage.

where E_G, E_{Si-V}, and E_{VF} are the band gap energy, energy interval between the Si $2p_{3/2}$ and the valence band maximum, and the valence band maximum scaled from the Fermi level, respectively. Here, $E_B + \Delta E_B$ is equal to $E_{VF} + E_{Si-V}$. Figure 10 indicates the valence band spectra taken at photon energy of 40 eV for the clean 6*H*-SiC(0001)-$\sqrt{3} \times \sqrt{3}$ surface (lower) and the Ta-sample holder (upper). The E_{VF} value is estimated to be 2.3±0.2 eV, which is compatible with that reported by Johansson *et al.*[14]. If one takes the E_G value of 2.83 eV for n-type 6*H*-SiC(0001) reported by Waldrop [15], the SBH values are deduced. Figure 11 shows the $\Phi_B{}^n$ values as a function of Ni coverage. The $\Phi_B{}^n$ value increases with increasing the Ni coverage and for Ni coverages of 3 and 5 ML it reaches the Schottky limit of 1.37 eV, which was reported by Hara [16]. Here, it must be noted that $\Phi_B{}^n + \Phi_B{}^p = E_G$ ($\Phi_B{}^p$: SBH for p-type semiconductor). The above result on SBH suggests an almost ideal contact of the ultrathin Ni layers and the clean 6*H*-SiC(0001) surface.

V. CONCLUSION

The ultra-thin Ni layers deposited at RT on the clean 6*H*-SiC(0001)-$\sqrt{3}\times\sqrt{3}$ surface were analyzed *in situ* by RHEED, high-resolution MEIS and SR-PES. The Ni(111) layers are grown uniformly and epitaxially at RT in spite of a large lattice mismatch of 20 %. The crystalline Ni layer consists of two types of small domains, (A) Ni-[110]// SiC-[1120] and (B) Ni-[112]//SiC-[1120] and the occupation ratio of (A) to (B) is 5 : 1. The streaky RHEED lines indicate a small size of the domains estimated to be several hundreds Å in lateral scale. Such an epitaxial growth of small size domains is probably due to the flat and narrow terraces of the SiC(0001) surfaces prepared in the present experiment(see Fig. 1(right)). It is interesting to try to stack Ni layers on an atomically flat SiC(0001) surface with wide terraces, which is obtained by annealing at high temperatures in H_2 or HCl ambiance[17,18]. The MEIS analysis shows that a small amount of Si are segregated to the surface and the crystalline Ni layer contains Si atoms (3-15 at %). The segregation rate is derived to be 0.015 s^{-1} by solving a simple rate equation. We also found a significant expansion of the inter-planar distance of Ni(111), which relaxes with increasing the Ni thickness. Such uniform stacking and epitaxial growth of Ni layers at RT may be responsible for surfactantlike Si atoms. The above two Si components are clearly observed in the Si *2p* core level spectra. The Si atoms contained in Ni layers show a higher binding energy shift by 0.4±0.1 eV than the Si atoms on top of the surface, indicating an electronic charge transfer from Si to Ni in the Ni lattice. The above relative binding energy shifts of Si *2p* are similar to those observed for the Ni disilicide and Si substrate of $NiSi_2$/Si(111) but not simply explained by the electronegativity of Si and Ni. The binding energy shift of the Si *2p* of the bulk SiC gives the Schottky barrier height, which increases with increasing Ni coverage and reaches the Schottky limit for the thickness more than 3 ML. This suggests an almost ideal contact of ultrathin Ni layers and the clean 6*H*-SiC(0001) surface.

References

1. J.E. Northrup and J. Neugebauer, Phys. Rev. **B52**, R17001 (1995).
2. U. Starke, J. Schardt, J. Bernhardt, M. Franke, and K. Heinz, Phys. Rev. Lett. **82**, 2107 (1999).
3. Y. Kido, H. Namba, T. Nishimura, A. Ikeda, Y. Yan, and A. Yagishita, Nucl. Instrum. Methods **B135-138**, 798 (1998).
4. T. Nishimura, A. Ikeda, and Y. Kido, Rev. Sci. Instrum. **69**, 1671 (1998).
5. Y. Kido, T. Nishimura, Y. Hoshino, and H. Namba, Nucl. Instrum. Methods **B161- 163**, 371 (2000).
6. W. Kern and D.A. Puotinen, RCA Review **31**, 187 (1970).

7. Y. Hoshino, O. Kitamura, T. Nakada, and Y. Kido, Surf. Sci. **539**, 14 (2003).
8. K. Kimura, Y. Endoh, and M. Mannami, Appl. Phys. Lett. **69**, 67 (1996).
9. M.H. Hoegen, J. Falta, M. Copel, and R.M. Tromp, Appl. Phys. Lett. **66**, 487 (1995).
10. H.-J. Gossmann, in *Delta-doping of Semiconductors*, ed. E.F. Schubert (Cambridge Univ. Press, Cambridge, 1996), p. 161.
11. E.L. Ballock, R. Gunnella, L. Patthey, T. Abukawa, S. Kono, C.R. Natori, and L.S.O. Johansson, Phys. Rev. Lett. **74**, 2756 (1995).
12. Z. Liu, S. Sugata, K. Yuge, M. Nagasono, K. Tanaka, and J. Kawai, Phys. Rev. **B** in press.
13. K.A. Mäder and H von Känel, Phys. Rev. **B48**, 4364 (1993).
14. L.I. Johansson, F.Owman and P. Mårtensson, Phys. Rev. **B53**, 13793 (1996).
15. J.R. Waldrop, J. Appl. Phys. **75**, 4548 (1994).
16. S. Hara, Surf. Sci. **494**, L805 (2001).
17. Q. Xue, Q.K. Xue, Y. Hasegawa, I.S.T. Tsong, and T. Sakurai, Appl. Phys. Lett. **74**, 2468 (1999).
18. S. Nakamura, T. Kimoto, H. Matsunami, S. Tanaka, N. Teraguchi, and A. Suzuki, Appl. Phys. Lett. **76**, 3412 (2000).